

Electronic Supplementary Information (ESI) for

High Performance Catalyst of Shape-specific Ruthenium Nanoparticles for Production of Primary Amines by Reductive Amination of Carbonyl Compounds

Debraj Chandra,^{*a} Yasunori Inoue,^{bc} Masato Sasase,^{cd} Masaaki Kitano,^{cd} Asim Bhaumik,^e Keigo Kamata,^b Hideo Hosono^{bcd} and Michikazu Hara^{*bcf}

^a World Research Hub Initiative (WRHI), Institute of Innovative Research, Tokyo Institute of Technology, Nagatsuta-cho 4259, Midori-ku, Yokohama 226-8503, Japan. E-mail: chandra.d.aa@m.titech.ac.jp

^b Laboratory for Materials and Structures, Institute of Innovative Research, Tokyo Institute of Technology, Nagatsuta-cho 4259, Midori-ku, Yokohama 226-8503, Japan. E-mail: mhara@mssl.titech.ac.jp

^c ACCEL, Japan Science and Technology Agency, 4-1-8 Honcho, Kawaguchi, Saitama, 332-0012, Japan.

^d Materials Research Center for Element Strategy, Tokyo Institute of Technology, Nagatsuta-cho 4259, Midori-ku, Yokohama 226-8503, Japan.

^e Department of Materials Science, Indian Association for the Cultivation of Science, 2A & B Raja S. C. Mullick Road, Jadavpur, Kolkata - 700 032, India.

^f Advanced Low Carbon Technology Research and Development Program (ALCA), Japan Science and Technology Agency (JST), 4-1-8 Honcho, Kawaguchi, Saitama 332-0012, Japan.

Contents

Experimental Detail

Table S1: Reductive amination of furfural (**1a**) over different Ru-NP catalysts.

Figure S1: XPS spectrum recorded on Ru 3d and Ca 2p region for Ru nanoparticles (Ru-NP) prepared from 10 wt% Ru-loaded Ca(NH₂)₂.

Figure S2: XPS spectrum recorded on N 1s region for Ru nanoparticles (Ru-NPs) prepared from different Ru-loaded Ca(NH₂)₂.

Figure S3: TEM image of 10 wt% Ru-loaded Ca(NH₂)₂ sample.

Figure S4: HRTEM image of Ru-NPs prepared from 20 wt% Ru-deposited Ca(NH₂)₂.

Figure S5: TEM, HRTEM images and XRD patterns of Ru-HCP sample.

Figure S6: Plot of the relative rate vs equiv of 1,10-phenanthroline per equiv of total Ru present for catalytic reductive amination of furfural over Ru-NP, Ru/Nb₂O₅ and Ru-HCP catalysts.

Figure S7: Reuse experiment of Ru-NP catalyst for the reductive amination of **1a** to **2a**.

Figure S8: Difference DRIFT spectra for adsorption of CO at -170 °C onto Ru-NPs prepared from different Ru-loaded Ca(NH₂)₂.

Figure S9: Computational free energy diagram for the possible pathways of reductive amination of furfural (**1a**) to furfurylamine (**2a**) and related side reaction.

Experimental Detail

Materials. Ca metal (99.99%), Ru₃(CO)₁₂ (99%), Ru(acac)₃, PVP (MW ~29000), ammonia solution (2M, in methanol) and 5-hydroxymethylfurfural (HMF) were purchased from Sigma-Aldrich. HNO₃ were obtained from Wako Chemical Co. Furfural and benzyl alcohol were purchased from TCI Chemicals. All other chemicals, unless mentioned otherwise, used in this investigation were of analytical grade. All the solutions were prepared by distilled water.

Synthesis of shape-specific flat Ru NPs. 10–20 wt% Ru-loaded Ca(NH₂)₂ samples were prepared by chemical vapor deposition using Ru₃(CO)₁₂ in accordance with a previous report.^{S1}
^{S2} The pristine Ru nanoparticles were prepared by acidic treatment of Ru-loaded Ca(NH₂)₂, through dissolution of Ca(NH₂)₂ support. In a typical procedure, 15 mL of 2-propanol was added to 2.0 g of Ru-loaded Ca(NH₂)₂ in a Ar-filled glovebox. Then to the mixture (pH >13) under stirring outside the glovebox, 2M HNO₃ was added dropwise and a stable pH≈4.0 was maintained. After adding 20 mL of water, the mixture was allowed to stir for another 2-4 h at 60 °C. The precipitate was recovered by centrifugation at 10000 rpm and washed repeatedly with water until neutral pH of centrifugate was achieved. Finally the sample was dried at 353 K and denoted as Ru-NP. Two reference supported metal catalysts of Ru deposited on Nb₂O₅ and SiO₂ (denoted as Ru/Nb₂O₅ and Ru/SiO₂, respectively) were prepared according to the previous report.^{S3} A control catalyst of conventional unsupported hcp Ru nanoparticles (denoted as Ru-HCP) was also prepared according to the literature^{S4} and the nanoparticles were characterized (Figure S5). In a typical procedure, synthesis was carried out in a 18 mL autoclave reactor with a Teflon vessel. Ru(acac)₃ (0.24 mmol; 95.6 mg) and PVP (100 mg) were dissolved in 10 mL of benzyl alcohol. The solvothermal reaction was kept at 150 °C for 24 h. After cooled down to room temperature, 40 mL acetone was added, and the nanoparticles were recovered by centrifugation at 10000 rpm for 10 min.

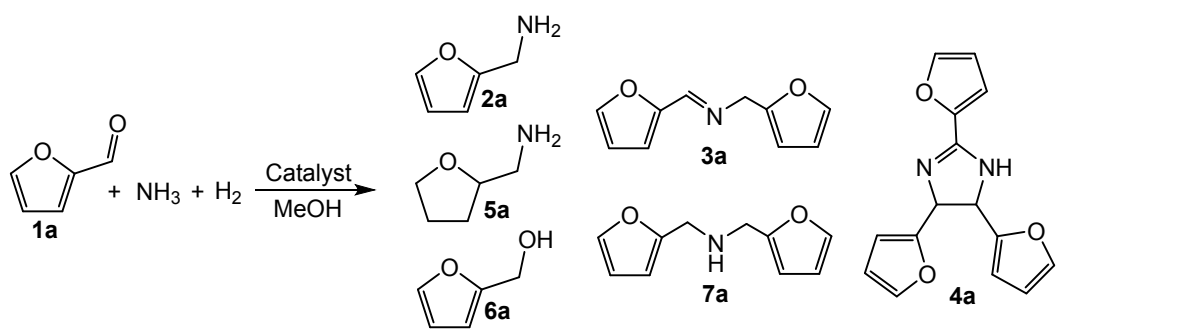
Structural characterizations. Powder X-ray diffraction (XRD) patterns were recorded on a diffractometer (Ultima IV, Rigaku; Cu K α , $\lambda = 1.5405 \text{ \AA}$, 40 kV–40 mA) equipped with a high-speed 1-dimensional detector (D/teX Ultra, Rigaku). Diffraction data were collected in the range of $2\theta = 10\text{--}80^\circ$ in 0.02° steps with a scan rate of $20^\circ/\text{min}$. Nitrogen adsorption-desorption isotherms were measured at 77 K with a surface area analyzer (Nova-4200e, Quantachrome). Prior to measurement, the samples were degassed under vacuum for 4 h at 353 K. The Brunauer-Emmett-Teller (BET) method was utilized to calculate the specific surface areas. The Ru dispersion were determined by CO pulse chemisorption at 323 K with a He flow of 30 mL min^{-1} and 0.09 mL pulses of 9.88% CO in He using a catalyst analyzer (BELCAT-A, MicrotracBEL); a stoichiometry of CO/Ru = 0.6 was assumed. The samples were reduced at 353 K (Ru-NP and Ru-HCP) for 10 h and 673 K (Ru/Nb $_2$ O $_5$ and Ru/SiO $_2$) for 2 h under H $_2$ flow (50 mL min^{-1}) before CO-pulse chemisorption. High-angle annular dark-field scanning transmission electron microscopy (HAADF-STEM) images were captured using a microscope (JEM-ARM 200F, Jeol) operated at 200 kV. Transmission electron microscopy (TEM) images were obtained using a microscope (JEM-2100F, Jeol) operated at 200 kV. X-ray photoelectron spectroscopy (XPS; ESCA-3400HSE, Shimadzu) was performed using Mg K α radiation (1253.6 eV) at 10 kV and 25 mA. Samples were pressed to fix on a thin metallic indium bed. The binding energies were calibrated using the Au 4f $_{7/2}$ peak, appearing at 83.0 eV. Diffuse reflectance infrared Fourier transform (DRIFT) spectra of CO adsorbed on the catalyst were measured using a spectrometer (FT/IR-6100, Jasco) equipped with a mercury–cadmium–tellurium detector at a resolution of 4 cm^{-1} . An alumina sample cup containing approximately 10 mg of catalyst was introduced into a water-cooled stainless steel heat chamber equipped with KBr windows (STJ-0123-HP-LTV, S.T. Japan). The samples were pretreated with H $_2$ gas flow (Ru-NP and Ru-HCP at 353 K for 8 h; Ru/Nb $_2$ O $_5$ and Ru/SiO $_2$ at 593 K for 2 h) and then cooled to room temperature. After the pretreatment, the sample was cooled to 103 K under vacuum to obtain a background spectrum. Pure CO (99.99999%) was supplied to the system at the same temperature. The difference FT-

IR spectra presented here were obtained by subtracting the backgrounds from the spectra of CO-adsorbed samples.

Catalytic reductive amination test. The catalytic reductive amination of various carbonyl compounds was conducted in an 18 mL autoclave reactor with a Teflon vessel containing a magnetic stirring bar. A Ru-NP dispersion was prepared by sonicating 10 mg Ru-NP powder in 10 mL methanol for 30 min; immediately followed by collection of 0.2 mL of this mixture under stirring and finally diluted to 1 mL by adding methanol. A typical procedure for the catalytic reductive amination of furfural was as follows. Furfural (0.5 mmol), Ru-NP dispersion (0.2 mg in 1 mL methanol), methanol solution of ammonia (4 mL, 8 mmol), and H₂ (2 MPa) were charged into the autoclave reactor. For Ru/Nb₂O₅ and Ru/SiO₂, 20 mg of catalysts were directly inserted and 1 mL methanol was added. The reactor was heated at 363 K for 0-6 h under continuous stirring. After completion of the reaction, reactor was allowed to cool down and then depressurized slowly. The catalyst was separated by filtration and the reaction solution was analyzed by gas chromatography (Shimadzu GC-17A) equipped with an InertCap 17 capillary column (internal diameter = 0.25 mm, length = 30 m) and with a flame ionization detector. For reuse experiment, after complete of the reaction the mixture was transferred in a round bottom flask and liquid part was removed by vacuum evaporation at 343 K. Residual catalyst on flask was dispersed in 1 mL of methanol by sonication and reused.

1,10-phenanthroline quantitative poisoning experiments for catalytic reductive amination of furfural. For each quantitative poisoning experiments with 1, 10-phenanthroline, a separate catalytic reductive amination test of furfural (as detailed above) was performed for different Ru NPs; except with one change: a quantitative, predetermined amount of 1, 10-phenanthroline was added to the initial solution. For this purpose, 0.03, 0.05, 0.08, 0.1 0.15, 0.2, 0.3 and 0.4 equivs of 1, 10-phenanthroline per total Ru was added for each separate poisoning experiment. Catalytic reaction was performed at 90 °C for 1 h with Ru-NP and 2 h with Ru/Nb₂O₅ and Ru-

HCP samples. The relative rate were determined; from the yield of furfurylamine (**2a**) obtained with different amount of 1, 10-phenanthroline, relative to that by without addition of 1, 10-phenanthroline.

Table S1. Reductive amination of furfural (**1a**) over different Ru nanoparticle catalysts^a

Entry	Catalyst ^b	Time (h)	p_{H_2} (MPa)	Yield ^c (%)					
				2a	3a	4a	5a	6a	7a
1	Ru-NP (10)	2	2	99	–	–	–	–	–
2	Ru-NP (15)	2	2	95	–	1	3	–	–
3	Ru-NP (20)	2	2	93	–	1	5	<1	1
4	Ru-HCP	2	2	39	49	4	5	–	<1
5	Ru-HCP	5	2	71	–	9	14	1	3
6 ^d	–	6	2	–	–	32	–	–	–

^a Reaction conditions: catalyst (0.2 mg), furfural (**1a**; 0.5 mmol), MeOH (5 mL), NH₃ (8 mmol), H₂ (2 MPa), 363 K. ^b Ru-NPs recovered from different wt% of Ru loaded on Ca(NH₂)₂ is shown in parenthesis. ^c GC yield. ^d Without catalyst.

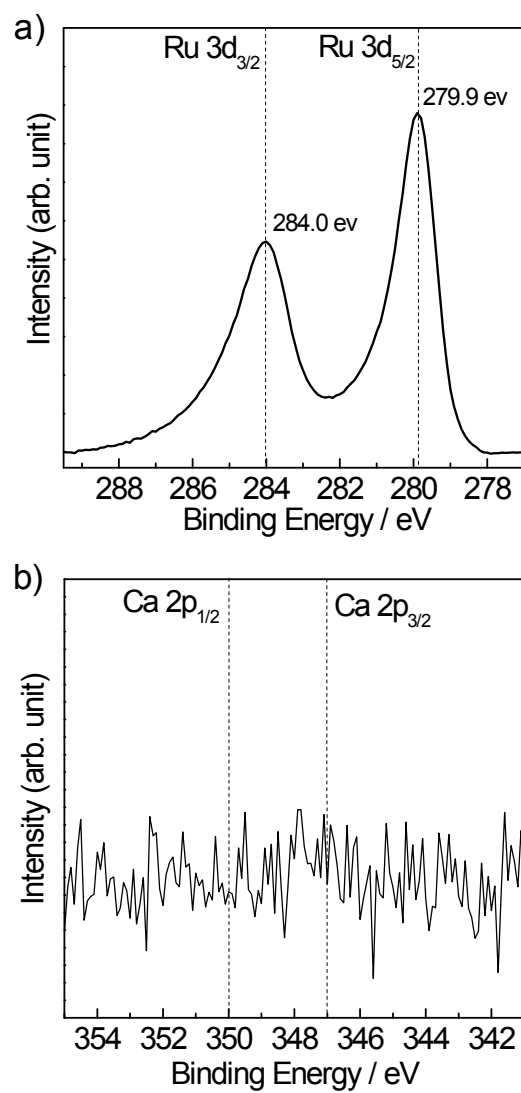


Figure S1. XPS spectrum recorded on (a) Ru 3d and (b) Ca 2p region for Ru nanoparticles (Ru-NP) prepared from 10 wt% Ru-loaded $\text{Ca}(\text{NH}_2)_2$.

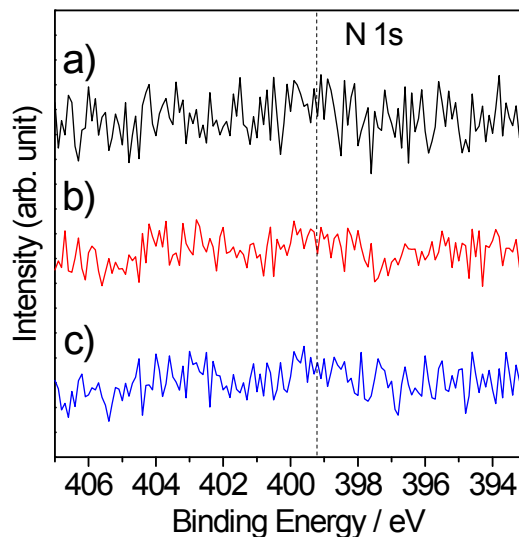


Figure S2. XPS spectrum recorded on N 1s region for Ru nanoparticles (Ru-NPs) prepared from (a) 10 wt%, (b) 15 wt% and (c) 20 wt% Ru-loaded Ca(NH₂)₂.

Note S1.

XPS spectrum recorded on N 1s region for different as-obtained Ru-NPs (Figure S2) depict lack of detectable peaks, which ruled out the presence of any trace of N element in the pristine Ru-NP catalysts. In Ru/Ca(NH₂)₂, a strong interaction between Ru-sites and N of basic Ca(NH₂)₂ persisted.^{S1} During acid treatment of Ru/Ca(NH₂)₂, dissolution of Ca(NH₂)₂ occurred through its transformation into water soluble Ca(NO₃)₂ and NH₄NO₃ species and thus interaction between Ru and basic N has been completely disappeared.

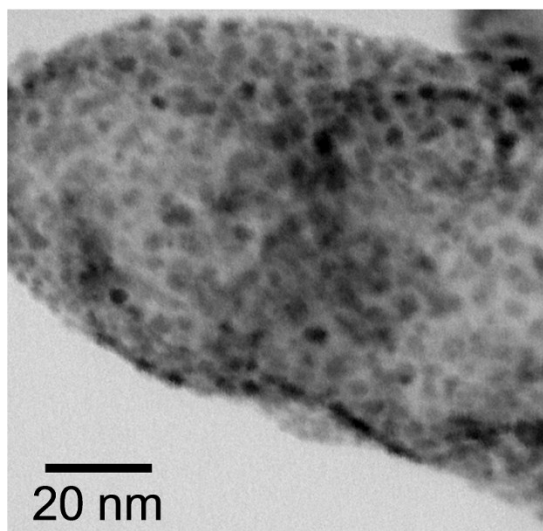


Figure S3. TEM image of 10 wt% Ru-loaded $\text{Ca}(\text{NH}_2)_2$ sample.

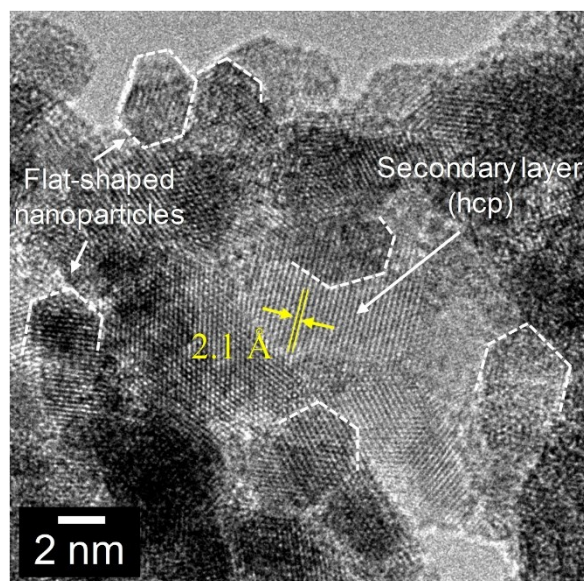


Figure S4. HRTEM image of Ru-NPs prepared from 20 wt% Ru-deposited $\text{Ca}(\text{NH}_2)_2$. Edges of few flat-shaped nanoparticles are highlighted by white dashed line.

Note S2.

HRTEM image (Figure S4) revealed that flat-shaped Ru NPs are intermingled with a large secondary layer. The lattice spacing in secondary layer were estimated to be 2.12 Å, which is in agreement with the conventional hexagonal-close-packed (hcp) structure ($d_{002} = 2.142$ Å) of Ru.^{S5, S6}

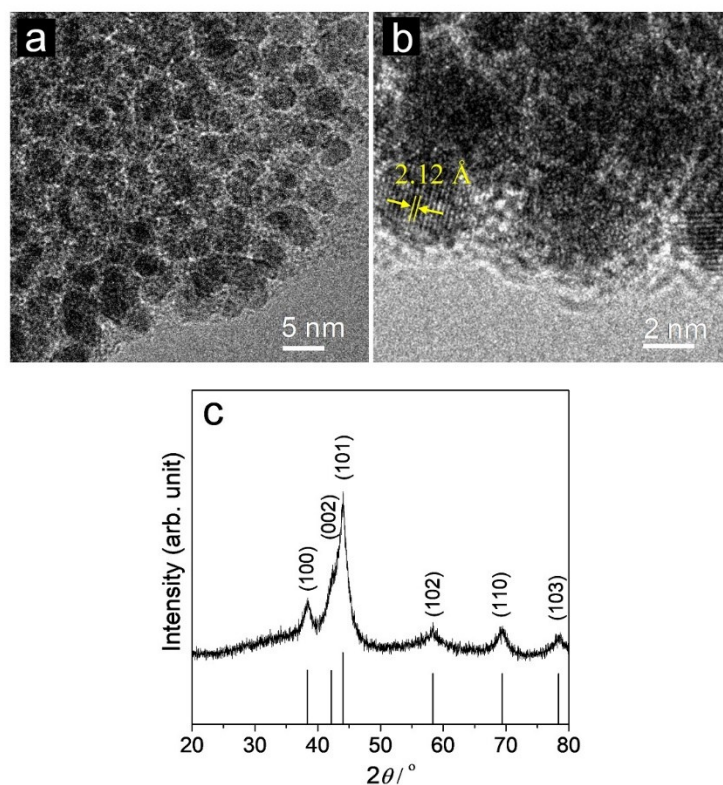


Figure S5. (a) TEM, (b) HRTEM images and (c) XRD patterns of Ru-HCP sample. JCPDF card number for XRD is 01-070-0274.

Note S3.

TEM image of Ru-HCP catalyst (Figure S5, a) shows uniformly dispersed nanoparticles of dimension ca. 5-6 nm. The lattice spacing in the Ru-HCP (Figure S5, b) were observed to be 2.12 Å, which is in agreement with the conventional hexagonal-close-packed (hcp) structure ($d_{002} = 2.142 \text{ \AA}$) of Ru particles.^{S5, S6} XRD pattern (Figure S5, c) also confirms the bulk structure of Ru-HCP as hcp Ru.

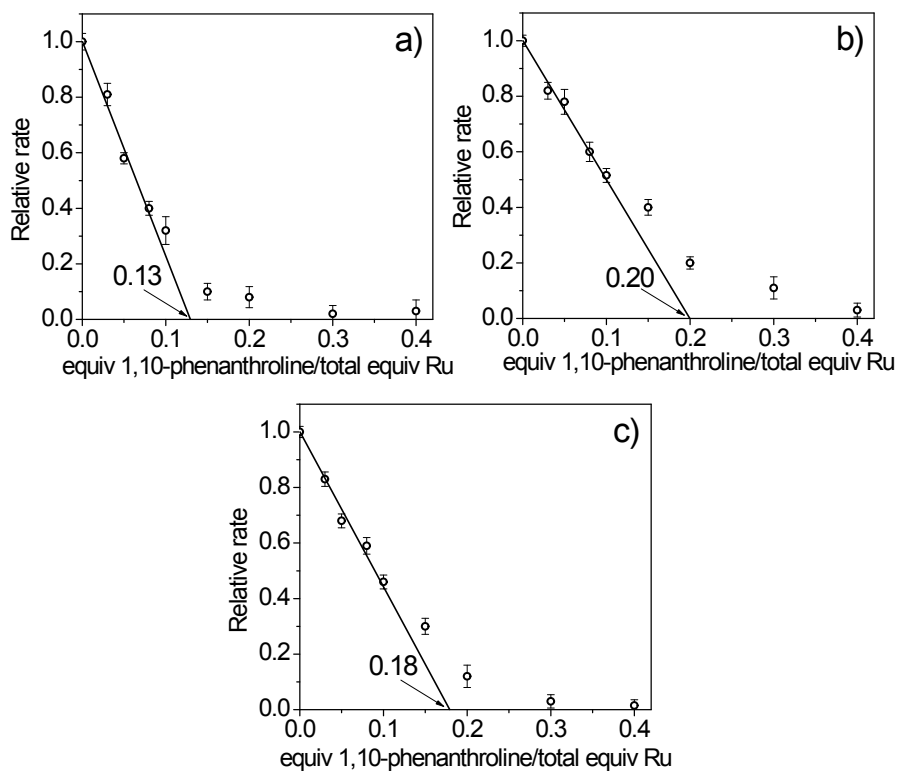


Figure S6. Plot of the relative rate vs equiv of 1,10-phenanthroline per equiv of total Ru present for catalytic reductive amination of furfural over (a) Ru-NP, (b) Ru/Nb₂O₅ and (c) Ru-HCP catalysts.

Note S4.

Analysis of quantitative poisoning experiment of different Ru catalysts. The quantitative catalyst poisoning studies using 1,10-phenanthroline^{S7, S8} has been employed to determine the TOF, based on actual number of catalytically active Ru-sites for the reductive amination of **1a**. The quantitative poisoning plot of Ru-NP, Ru/Nb₂O₅ and Ru-HCP with 1,10-phenanthroline is given in Figure S6. The relative rate initially decreases linearly with increasing number of poison equiv, as is commonly seen in the literature,^{S7, S8} which implies a strong association between the Ru-sites and 1,10-phenanthroline. Hence, in the linear region, the initial 1,10-phenanthroline concentration will be equal to the poisoned catalyst concentration, that is, [1,10-phenanthroline]_{initial} \approx m [{Ru-(1,10-phenanthroline)_m}. The poisoning data were analyzed

by drawing straight lines to the linear portion of the plot to find $x_{\text{intercept}}$, which is the required equivalent of 1,10-phenanthroline per total equiv of metal needed to deactivate the catalyst completely. By assuming $m \approx 1$, at lower initial 1,10-phenanthroline concentration, the $x_{\text{intercept}}$ give the fraction of Ru-sites present in the catalysts. The $x_{\text{intercept}}$ for the Ru-NP, Ru/Nb₂O₅ and Ru-HCP were found to be 0.13, 0.2 and 0.18, respectively. The TOFs for the formation **2a**, estimated using the $x_{\text{intercept}}$ values were 1580 h⁻¹, 370 h⁻¹ and 270 h⁻¹ for Ru-NP, Ru/Nb₂O₅ and Ru-HCP, respectively. The result indicate the smaller fraction of catalytic Ru-sites are present in Ru-NP compared to those of Ru/Nb₂O₅ and Ru-HCP, which is in agreement with the dispersion of surface Ru atoms obtained from CO chemisorption (Table 1). However, the exceedingly higher TOF for **2a** over Ru-NP revealed that the Ru-sites persist on the surface of Ru-NP are highly active.

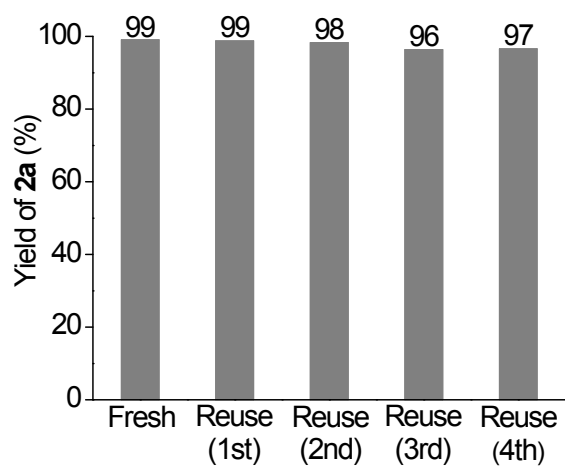


Figure S7. Reuse experiment of Ru-NP catalyst for the reductive amination of **1a** to **2a**.

Reaction conditions: Catalyst (0.2 mg), **1a** (0.5 mmol), MeOH (5 mL), NH₃ (8 mmol), and H₂ (2 MPa), 363 K, 2 h.

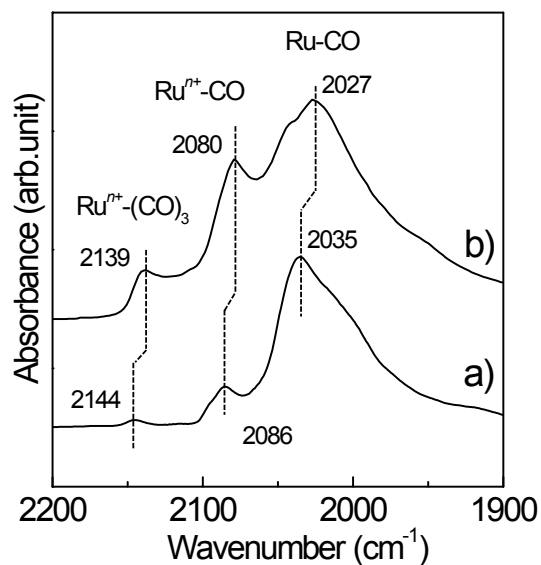


Figure S8. Difference DRIFT spectra for adsorption of CO at $-170\text{ }^{\circ}\text{C}$ onto Ru-NPs prepared from (a) 10 wt% and (b) 20 wt% Ru-loaded $\text{Ca}(\text{NH}_2)_2$.

Note S5.

When CO was adsorbed on Ru-NP (20), a band was observed at 2027 cm^{-1} with a shoulder (ca. 2035 cm^{-1}) assignable to CO adsorbed on flat-shaped fcc Ru NPs (Figure S8). These results suggest that flat-shaped Ru NPs are mixed with large hcp Ru NPs in Ru-NP (20); Ru-NP (20) has a higher TOF than Ru-HCP (Table 1) although the diffraction peaks due to hcp Ru are mainly observed in the XRD pattern for Ru-NP (20).

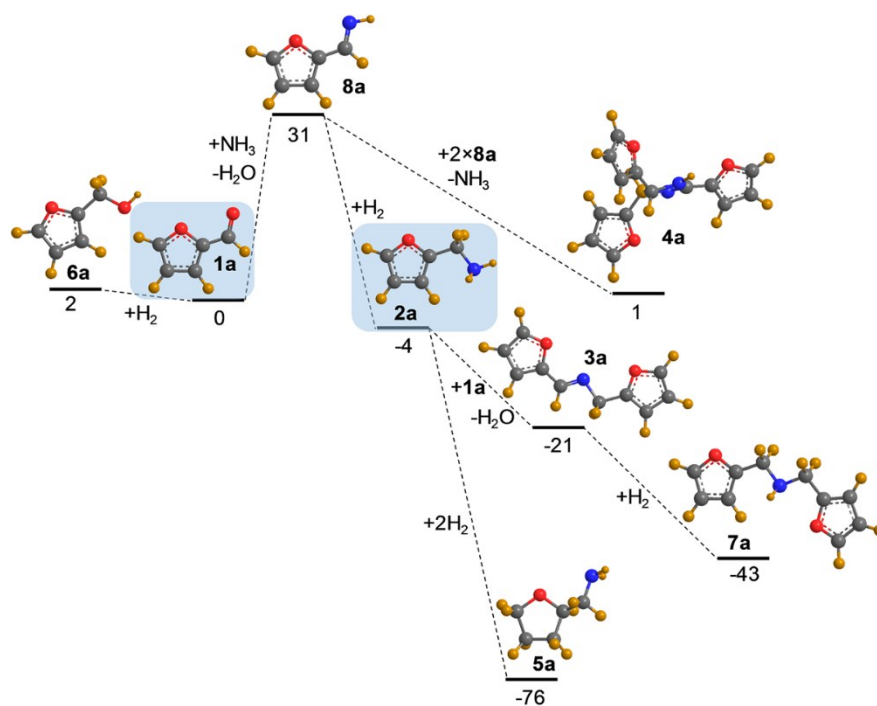


Figure S9. Computational free energy diagram for the possible pathways of reductive amination of furfural (**1a**) to furfurylamine (**2a**) and related side reaction. Dotted lines shows the possible reaction pathways. C, O, N and H atoms are represented by gray, red, blue and yellow spheres, respectively. Energies are shown in kJ mol^{-1} and based on **1a**, calculated using density functional theory (DFT).^{S3}

Note S5.

Computational free energy diagram for possible pathways for the reaction of furfural (**1a**) in the presence of NH_3 and H_2 is described in Figure S6.^{S3, S9, S10} Furfurylamine (**2a**) is a valuable primary amine in biorefineries because **1a** is readily accessible from biomass.^{S11, S12} Reductive amination of **1a** proceeded through the unstable intermediate furfurylimine (**8a**). Formation of primary amine **2a** was determined to be more thermodynamically unfavorable than that of secondary amine (**7a**) and undesired hydrogenated product (**5a**) according to their computational free energies,^{S3} which indicates the difficulty in the selective synthesis of primary amines. *N*-furfurylidene-furfurylamine (**3a**), 2,4,5-tris (2-furyl)imidazoline (**4a**),

tetrahydrofurfurylamine (**5a**), furfuryl alcohol (**6a**) and difurfurylamine (**7a**) are the main byproducts.

References

- S1. Y. Inoue, M. Kitano, K. Kishida, H. Abe, Y. Niwa, M. Sasase, Y. Fujita, H. Ishikawa, T. Yokoyama, M. Hara and H. Hosono, *ACS Catal.*, 2016, **6**, 7577-7584.
- S2. M. Kitano, Y. Inoue, Y. Yamazaki, F. Hayashi, S. Kanbara, S. Matsuishi, T. Yokoyama, S.-W. Kim, M. Hara and H. Hosono, *Nat. Chem.*, 2012, **4**, 934-940.
- S3. T. Komanoya, T. Kinemura, Y. Kita, K. Kamata and M. Hara, *J. Am. Chem. Soc.*, 2017, **139**, 11493-11499.
- S4. W.-Z. Li, J.-X. Liu, J. Gu, W. Zhou, S.-Y. Yao, R. Si, Y. Guo, H.-Y. Su, C.-H. Yan, W.-X. Li, Y.-W. Zhang and D. Ma, *J. Am. Chem. Soc.*, 2017, **139**, 2267-2276.
- S5. J. Ohyama, T. Sato, Y. Yamamoto, S. Arai and A. Satsuma, *J. Am. Chem. Soc.*, 2013, **135**, 8016-8021.
- S6. A.-X. Yin, W.-C. Liu, J. Ke, W. Zhu, J. Gu, Y.-W. Zhang and C.-H. Yan, *J. Am. Chem. Soc.*, 2012, **134**, 20479-20489.
- S7. E. Bayram, J. C. Linehan, J. L. Fulton, J. A. S. Roberts, N. K. Szymczak, T. D. Smurthwaite, S. Özkar, M. Balasubramanian and R. G. Finke, *J. Am. Chem. Soc.*, 2011, **133**, 18889-18902.
- S8. E. Bayram and R. G. Finke, *ACS Catal.*, 2012, **2**, 1967-1975.
- S9. M. Chatterjee, T. Ishizaka and H. Kawanami, *Green Chem.*, 2016, **18**, 487-496.
- S10. S. Nishimura, K. Mizuhori and K. Ebitani, *Res. Chem. Intermed.*, 2016, **42**, 19-30.
- S11. A. Corma, S. Iborra and A. Velty, *Chem. Rev.*, 2007, **107**, 2411-2502.
- S12. M. Hara, K. Nakajima and K. Kamata, *Sci. Technol. Adv. Mater.*, 2015, **16**, 034903.